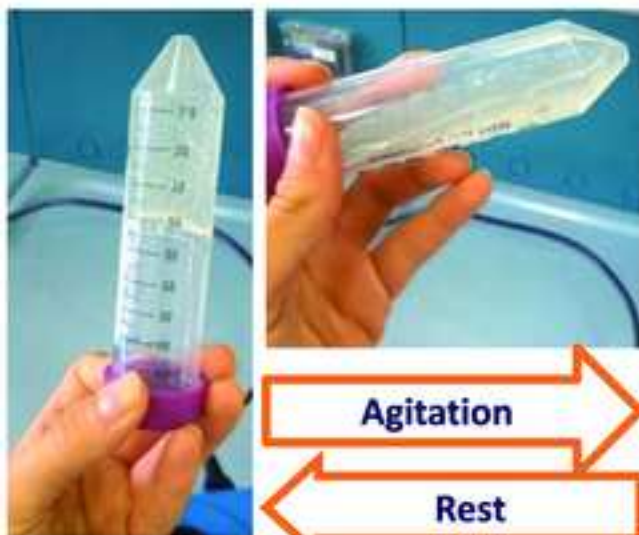
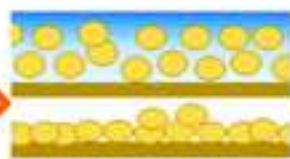


# SILK FIBROIN HYDROALCOHOLIC GELS



**Thixotropy**

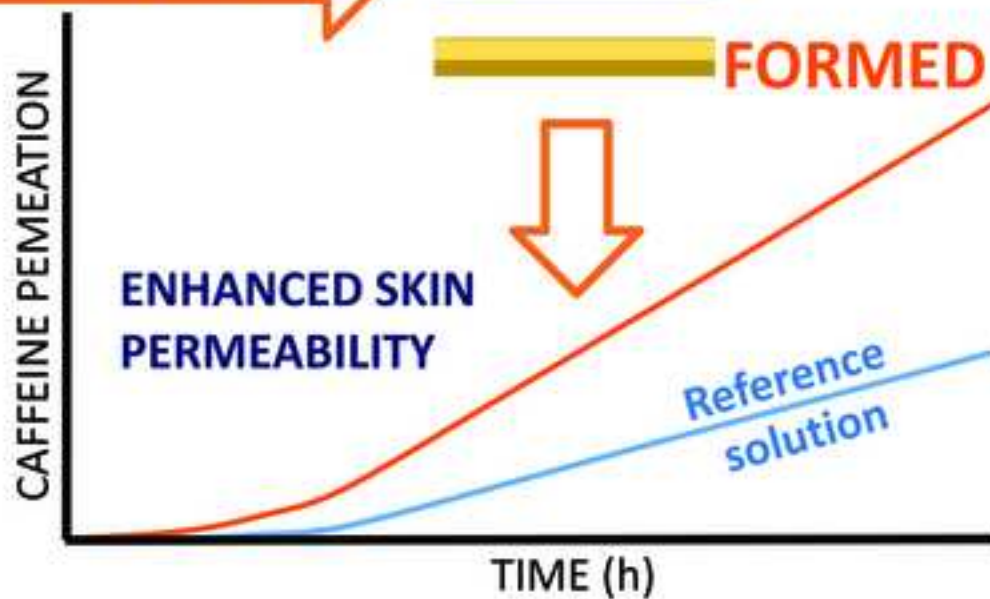
Easy to spread on the skin



Fast evaporation



**FORMED FILMS**



# In situ film forming fibroin gel intended for cutaneous administration

Chiara G.M. Gennari<sup>1</sup>, Francesca Selmin<sup>1</sup>, Marco A. Ortenzi<sup>2</sup>, Silvia Franzé<sup>1</sup>, Umberto M. Musazzi<sup>1</sup>, Antonella Casiraghi<sup>1</sup>, Paola Minghetti<sup>1</sup>, Francesco Cilurzo<sup>1\*</sup>

<sup>1</sup> Department of Pharmaceutical Sciences, Università degli Studi di Milano, Via G. Colombo, 71 - 20133 Milan, Italy

<sup>2</sup> Department of Chemistry, CRC Materiali Polimerici (LaMPo), Università degli Studi di Milano, Via Golgi, 19 - 20133 Milan, Italy

\* To Whom the correspondence should be sent:

Prof. Francesco Cilurzo, PhD  
Department of Pharmaceutical Sciences  
Università degli Studi di Milano  
Via G. Colombo, 71 -20133 Milan, Italy  
Phone: + 39 02 503 24635  
Fax: + 39 02 503 24657  
e-mail: francesco.cilurzo@unimi.it

## **Abstract**

The possible use of regenerated silk fibroin gels as in situ film forming formulations for cutaneous administration of drugs was studied. Ethanol was selected as volatile and skin tolerant solvent to favor the sol-gel transition of silk fibroin solutions. Glycerin was chosen to ameliorate the gel texture profile. Eighteen placebo formulations were prepared to individuate the optimal component ratios as a function of the texture analysis, spreadability and drying time. The in vitro biopharmaceutical performance was investigated by in vitro permeation test through human epidermis loading caffeine as a model drug. The data evidenced that the optimal technological performances were achieved using gels containing 70 % ethanol and silk fibroin/glycerin ratio from **0.18 to 0.36**. The caffeine flux ( $J$ ) through the skin was significantly improved due to an increase of the drug thermodynamic activity (hydro-alcoholic solution:  $J \sim 0.8 \mu\text{g}/\text{cm}^2/\text{h}$ ; in situ formed film:  $J \sim 1.4\text{-}1.7 \mu\text{g}/\text{cm}^2/\text{h}$ ). In conclusion, silk fibroin can be advantageously proposed as a novel film forming material to develop dosage forms to be topically applied.

## **Keywords:**

Silk fibroin; texture analyses; thixotropic gel; skin penetration enhancement; in situ film forming; caffeine

## 1. Introduction

In situ film forming polymeric dispersions have been proposed as a novel approach to deliver drugs through the skin. These dispersions generally consist in a very simple formulation comprising a drug substance, a film-forming polymer and a volatile skin tolerant solvent. They are applied and/or sprayed onto the skin as liquids or gels forming in situ a very thin polymeric film after the rapid solvent evaporation.

With respect to other topically-applied dosage forms, they offer an improved flexibility in dosage, easiness in use, reduced irritation potential, superior cosmetic appearance without leaving greasy feeling on the application site and a simplicity of manufacturing and scalability. Moreover, in situ film forming polymeric dispersions can enhance the drug skin penetration since the fast solvent evaporation may lead the formation of a supersaturated system, which favours the drug partition from the dosage form towards the skin, having a greater thermodynamic activity with respect to saturated system (Cilurzo et al., 2015).

Although this enhancement strategy was successfully proposed in the development of transdermal patches (Minghetti et al., 2007) or medicated plasters (Cilurzo et al., 2010), the physical stability of the loaded drug over the entire product validity (i.e., at least 2 years) represents a very critical issue due to the presence of a supersaturated system (Kim and Choi, 2002). By contrast, in the case of in situ film forming dosage forms, the drug physical stability is a matter of few hours, namely the application time.

The feasibility of formulating in situ film forming dosage forms has been demonstrated by using different polymers, such as methyl methacrylate copolymers, cellulose ethers, poly(vinyl pyrrolidone)s or mixtures thereof, dispersed usually in organic solvents or in some cases in aqueous media (Cilurzo et al., 2014).

Silk fibroin is a naturally occurring protein extracted from the silkworm *Bombyx mori* cocoons and shaped into films (Hofmann et al., 2006), gels (De Moraes et al., 2015; Pritchard et al., 2013), microspheres (Cilurzo et al., 2011), under mild and all-aqueous conditions (Selmin et al., 2014). **In particular, silk fibroin films in the wet state present oxygen and water vapor permeability, similar to those of human skin (Vepari and Kaplan, 2007).**

**Films made of regenerated silk fibroin as such suffer two main drawbacks, namely solubility in aqueous medium and brittleness. A common method to solve the issue of water solubility consists in the treatment with dehydrating alcohols. However, this final cure can determine a further increase of the film brittleness (Nazarov et al., 2004). To improve mechanical properties and obtain more flexible films, the use of plasticizers is therefore mandatory (Jin et al., 2005; Dai et al., 2002; Lu et al., 2010). Among them, glycerin was previously reported to improve silk fibroin mechanical properties by adding a plasticizer solution during film formation (Kawahara et al., 2006). In particular, a glycerin content higher than 20% w/w led water-insoluble and flexible films (Lu et al., 2010).**

**Beside the possibility to prepare a fibroin water-insoluble film with suitable mechanical characteristics, the use of this protein appears of interest due to its self-assembly properties which can be exploited to control the sol-gel transition which can be advantageously use to design an in situ film forming dosage**

form. The sol-gel transition can be modulated by variation of pH and ionic strength and the addition of organic solvents (Kim et al., 2004; Matsumoto et al., 2006; De Moraes et al., 2015) as well as physical treatment such as heating and sonication (Wang et al., 2005; Wang et al., 2008).

40 On the bases of these considerations, the present work explored the possible use of silk fibroin gel as in situ film forming formulation for cutaneous administration of drugs using ethanol, a volatile and skin tolerant solvent, to favor the sol-gel transition of silk fibroin solutions (De Moraes et al., 2015). To pursue this aim, the textural properties of the silk fibroin gels were investigated since they have direct relevance to their performances. Ideally, these formulations should be designed in order to minimize the hardness and maximize the adhesiveness and the cohesiveness. The hardness, i.e. the force required to provide the  
45 deformation of a gel formulation, also expresses the applicability of a gel to the desired site. A low hardness value can be advantageous exploited for the cutaneous application of formulations since it significantly influences the spreadability of the gel as film mold. In other words, the lower the hardness of the gel, the higher the spreadability. The gel adhesive properties are related to the permanence of the preparation onto the skin surface. Finally, the cohesiveness is a measure of the degree of difficulty in breaking down the  
50 gel internal structure and, therefore, to overcome the stresses due to the body movements. Therefore, it is expected that high values of cohesiveness can favor the formation of homogeneous films.

The study was subdivided in two parts: the former examined the effects of the concentrations of silk fibroin, ethanol and plasticizer on the most critical parameters for an in situ film forming gel. The formulations presenting optimal texture properties and convenient drying time were then loaded with  
55 caffeine to investigate the in vitro skin permeation through human epidermis. Caffeine was chosen as a model drug since it is indicated as reference compound for in vitro permeation experiments by both OECD (OECD, 2004) and EMA (EMA, 2014). Moreover, it is reported to exhibit a relatively low permeability and lag-phase (van der Sandt et al., 2004).

## 60 2. Materials and Methods

### 2.1 Materials

Cocoons of *B. mori* silkworm were kindly supplied by ISMAC-CNR (Biella, Italy). Lithium bromide and glycerin were purchased from Carlo Erba Reagenti (Italy). Caffeine was supplied from Fluka (China) and  
65 ethanol was purchased from VWR International (Italy).

### 2.2 Fibroin regeneration

Degummed *B. mori* silk fibers were dissolved in 9.3 M LiBr at 70 °C for 3 h. Afterwards, the solution was centrifuged at 5000 rpm for 20 min to remove the silk aggregates, namely debris and environment  
70 contaminants usually presented on the cocoons. The resulting solution was then dialyzed in cellulose tube

(MWCO 12 kDa, Sigma-Aldrich, Italy) against distilled water for 2 days at room temperature to remove lithium bromide. The completion of the dialysis process was monitored by conductivity measurements (FiveEasy™, Mettler Toledo, Italy). Undissolved particles were then removed by centrifugation at 5000 rpm for 20 min. The aqueous silk fibroin dispersion was freeze-dried by an Epsilon 2-6 LSC (Martin Christ, Germany) as previously described (Selmin et al., 2014). Upon completion of drying process, hydro-dispersible silk fibroin was obtained.

### 2.3 Silk fibroin gel preparation

Aqueous dispersions of silk fibroin were prepared by dissolving the freeze dried material in water in order to obtain a concentration of 2, 3 or 4 % w/w and stirred overnight to ensure the complete dissolution of the protein. Ethanol was added to each silk fibroin solution in the following volume ratios (silk fibroin aqueous dispersion/ethanol): 70/30, 50/50 and 30/70 w/w. The final silk fibroin concentrations are reported in **Table 1**. Furthermore, amounts of glycerin ranging from 0 to 7.5% w/w were also added into the hydro-alcoholic silk fibroin dispersions (**Table 1**).

For the preparation of the drug loaded gels, caffeine was previously dissolved in ethanol to obtain a silk fibroin gel containing 1% w/w of caffeine. Then, the same procedure used for the preparation of placebo gels was applied.

### 2.4 Gel characterization

#### 2.4.1 Texture analysis

Silk fibroin gels were poured on small Petri dishes in order to obtain a final sample height of 1.3 cm. A compression test was carried out to evaluate the influence of the formulation variables (i.e., silk fibroin ethanol and plasticizer concentrations) on the gel mechanical performances. The samples were tested by using a 2712-041 Instron machine (Norwood, USA) equipped with a 50 N load transducer and sample data exported using Bluehill Software Version 3.31.

A flat stainless probe (5 mm diameter) was forced down into each sample at a defined rate (0.1 mm/s) and to a defined depth (66% of the sample height). At least five replicate analyses of each sample were performed at 25 °C.

#### 2.4.2 Rheological characterization

All rheological experiments were performed at 37±0.1 °C in the strain-controlled mode using a Physica MCR 300 rheometer (Anton Paar GmbH, Austria) using a cone-and-plate geometry of 1° incline, 25 mm diameter. To study the thixotropic properties of silk fibroin gels, two frequency sweep tests were performed using the same plate geometry on the sample: a first run from 0.1 to 100 Hz immediately followed by a second run from 100 to 0.1 Hz. Strain was set at 5% **in order to be in the linear viscoelastic**

**regime of the gel. In the present work**, shear rate ( $\dot{\gamma}$ ) and viscosity ( $\eta$ ) are used, passing from experimental data obtained as complex viscosity versus angular frequency to data as standard shear viscosity versus shear rate thanks to Cox-Merz rule.

#### 110 2.4.3 Qualitative evaluation of spreadability

Silk fibroin gels were spread at the thickness of 800  $\mu\text{m}$  on a backing layer by using a Mathis Labcoater Labdryer (Mathis, Switzerland). A preliminary assessment of the spreadability of film forming dispersions was evaluated according to the following scoring system based on a visual evaluation: *poor spreadability* (C) represents not spreadable formulations, *medium spreadability* (B) when the film was partly formed or with  
115 sporadic flaking or *good spreadability* (A) if the formed film was uniform without any failures.

#### 2.4.4 Drying time

The time required for the film formation after spreading a 800  $\mu\text{m}$  thick gel layer on a backing layer was evaluated in vitro by a gravimetric method. Even if this thickness is not representative of the in-use  
120 condition, it was selected to better discriminate the influence of the formulation composition on the drying time.

The formulations, maintained at 32 °C (i.e. the skin temperature), were weighed immediately after spreading and every 10 min over a 1 h period. The drying time was expressed as the time required to reduce the initial weight of the 85% ( $t_{ev}$ ).

125

#### 2.5 In vitro skin penetration study

The skin used for the preparation of the epidermal membrane was obtained from abdominal plastic surgery. After removing the subcutaneous fatty tissue the skin was kept frozen until further use. For the sample preparation, adequate pieces of the frozen skin were immersed in water of 60 °C for 60 s according  
130 to an internal protocol (Gennari et al., 2016). After this treatment, the epidermis was carefully removed from the underlying tissue with the help of forceps. The integrity of all tissue samples was assessed measuring their electrical resistance (voltage: 250 mV, frequency: 100 Hz; Agilent 4263B LCR Meter, Microlease, Italy). All samples were hydrated and sandwiched between the donor and receptor compartments of a modified Franz diffusion cell (PermeGear, USA) with an effective penetration area and a  
135 receptor volume of 0.636  $\text{cm}^2$  and 3 mL, respectively. The donor and receiver compartments were filled with physiologic solution. The system was kept at  $37\pm 1$  °C by means of a circulating water bath so that the skin surface temperature was at  $32\pm 1$  °C and the receiver medium was continuously maintained under stirring with a magnetic bar. Before the measurement, the samples were equilibrated for 30 min. Samples with an electrical impedance resistance higher than 40  $\text{K}\Omega\cdot\text{cm}^2$  were used for the in vitro permeation  
140 experiments (Franzé et al., 2015). Afterwards, the system was dismantled and the following donor phases

were applied on the epidermis sample: a) caffeine loaded silk fibroin gel; b) 1% w/v hydro-alcoholic caffeine solution; c) preformed caffeine loaded silk fibroin film.

The experiments (three replicates per formulation) were performed over a 24 h period under non-occlusive conditions, with the exception of the hydro-alcoholic solution. In this latter case, the experiment was performed sealing the donor compartment to avoid the solvent evaporation. During this period, 200  $\mu$ L samples were drawn at predetermined intervals and replaced by aliquots of the receptor fluid. Sink conditions were maintained throughout the experiment.

### 2.6 Caffeine quantification

Caffeine was quantified by an HPLC method (Agilent HP 1100 series, Chemstation Hewlett Packard, USA). The column used was an Accucore XL C18 (1000 x 4.6 mm, 4  $\mu$ m) at 25 $\pm$ 1  $^{\circ}$ C. The mobile phase was acetonitrile/water containing 0.1 % v/v acetic acid (10:90, % v/v). With a flow rate of 1 mL/min the retention time for caffeine was approximately 2.2 minutes. Caffeine was detected at 272 nm. The method provided good precision and linearity in the required concentration range (0.5 – 10  $\mu$ g/mL,  $R^2=0.9993$ ).

### 2.7 Statistical analysis

The effects of silk fibroin and ethanol on hardness ( $\sigma_{max}$ ), cohesiveness (AUC+) and adhesiveness ( $\sigma_{min}$ ) of silk fibroin gels were estimated by multiple linear regression using OriginPro 2015 (OriginLab Corporation, USA)

## 3. Results and discussion

**Figure 1** represents the typical stress/strain curve of a silk fibroin-based gel. The textural profiles displayed linearity preceding a plateau region, suggesting that the silk fibroin gels have viscoelastic characteristics. The analyses of the cycle permitted to calculate the maximum resistance of the gel to penetration by the probe ( $\sigma_{max}$ ), the corresponding work (AUC+), and the maximum negative force ( $\sigma_{min}$ ) registered during the withdrawal step. The value of AUC+ is an expression of the cohesiveness of the sample, while  $\sigma_{max}$  and  $\sigma_{min}$  correspond to sample hardness and adhesiveness, respectively (**Table 1**).

The influence of the concentrations of silk fibroin and ethanol on the AUC+,  $\sigma_{max}$  and  $\sigma_{min}$  of gels is represented in **Figures 2a-c**. The trends evidenced that at highest silk fibroin concentration, the values of all the textural properties were increased. All the three considered textural properties appeared linearly influenced by both the selected formulative variables (**Table 2**). Moreover, the contribute of silk fibroin concentration was the most significant since the coefficients of fibroin concentration in all the equations



175 resulted at least two order of magnitude higher than those found for the ethanol concentration. Considering that the evaporation rate of the formulations prepared with the highest ethanol concentration allowed the faster film formation ( $t_{ev}$ , formulations A1, A4, and A7, **Table 1**), the effect of the plasticizer was studied only using the silk fibroin gels prepared with the largest amount of alcohol.

The addition of 2.5% w/w or 5% w/w glycerin determined the formation of more coherent gels as demonstrated by the increase of AUC+ values (**Figure 3a**). Furthermore, a concomitant increase of the hardness was measured reaching the highest value in the case of the formulations containing 5% glycerin (**Figure 3b**). Finally, the addition of glycerin also improved the adhesiveness of the gels to the stainless steel punch during its removal (**Figure 3c**). All together, these data indicated that glycerin acted as stabilizer of the gel structure at the silk fibroin/glycerin ratio up to 0.5. Indeed, the AUC+,  $\sigma_{min}$  and  $\sigma_{max}$  of formulation G7 (**Table 3**) were not statistically different to those of the formulation A7 (**Table 1**).

180 Even if the addition of glycerin determined an increase of the gel textural properties, the spreadability was not still satisfying, as evidenced by the score system reported in **Table 3**. However, the manual agitation of some of the gels containing glycerin determined a significant improvement of the flowability suggesting that not only this component acted as a plasticizer, but also it induced a thixotropic behavior to the gel.

190 Therefore, the thixotropy was studied through frequency sweep experiments. The samples were first analyzed passing from low to high angular frequencies to break the gel structure and pass to sol structure. Then, they were analyzed passing from high to low angular frequencies without time lag between the two analyses in order to avoid the re-formation of a gel structure. As an example, the rheological pattern of formulation G4 is depicted in **Figure 4**. The difference in viscosity between the two curves is clearly marked as the value at low shear shifted from around 35.5 Pa\*s, when the gel structure was present, to about 9.5 Pa\*s when the sol was present. The gel structure was fully recovered after about 35 minutes.

195 Thus, the spreadability was re-evaluated after manual agitation of the formulations into the container (**Table 3**). On the bases of the qualitative score system, three general considerations can be drawn. First, the higher the silk fibroin content, the lower the spreadability. Secondly, to obtain a film with acceptable cosmetic properties, a silk fibroin/glycerin ratio lower than 0.48 was required (Formulation G7, **Table 3**).

200 Thirdly, only at the silk fibroin/glycerin ratios higher than 0.12, the agitation improved the flowability favoring the formation of a uniform and transparent film (**Table 3**). Indeed, in case of Formulations G2, G3 and G6, the agitation caused the formation of a sol so fluid that a significant shrinkage occurred during spreading.

205 As far as the drying time ( $t_{ev}$ ) is concerned, the higher the silk fibroin concentration, the higher the drying time (**Table 1** and **Table 3**). As expected, the influence of the highest ethanol concentration on the net evaporation at each time point was also evident. The formulations containing glycerin required a longer time period to dry than the corresponding systems without plasticizer. Moreover, the gels containing 7.5% w/w glycerin showed longer drying time than those prepared with 5% w/w or 2.5% w/w. Such effect could

210 be probably due to the hygroscopicity of glycerin, which reduces the evaporation rate of water. It should be also underlined that the trend in the  $t_{ev}$  values resulted similar to that found for AUC+ ( $R^2=0.77$ ), suggesting that the time required for the film formation was dependent not only on the formulation composition, but also on the gel cohesiveness: the more coherent the gel, the lower the evaporation rate.

On the basis of the main characteristics of the prepared films, formulations G1, G4 and G5 were considered 215 worth of further investigations since they represented the whole range of the silk fibroin/glycerin ratios that allowed silk fibroin gels with satisfactory technological properties (Formulation G1: 0.24; Formulation G4: 0.36; Formulation G5: 0.18).

The addition of 1% w/w caffeine to silk fibroin gels did not cause a significant modification of their technological characteristics (data not shown). **Figure 5** compares the permeation profiles through human 220 epidermis of caffeine from silk fibroin films and the reference hydro-alcoholic solution. As reported in **Table 4**, all in situ formed films showed higher fluxes than the reference solution ( $p<0.05$ ). To better understand the possible enhancement mechanism an in vitro permeation experiment was also carried out applying directly onto the human epidermis the pre-formed film obtained by drying the formulation G5. The results evidenced no differences in lag times and fluxes (**Table 4**), suggesting that ethanol did not enhance the 225 drug permeation probably because its evaporation rate was faster than its ability to penetrate the skin. On the other hand, the solvent removal increased the caffeine concentration in the formed film up to about 10-12%, determining an improvement of the drug thermodynamic activity in the formulation and, therefore, the drug flux.

Indeed, the inspection of the caffeine loaded films by optical microscopy revealed the absence of crystals. 230 In other words, the comparison of the fluxes obtained by the in situ formed films and hydro-alcoholic solution evidenced that the increased caffeine concentration within the silk fibroin film favors the partition from the film towards the stratum corneum (**Table 4**). And again, the difference in lag time length, also permitted to underline that the drug partition from the vehicle toward the stratum corneum appeared the limiting step more relevant than its diffusion through deeper layers of the human epidermis

235 The use of an organic solvent, such as ethanol, is the most common method to convert silk fibroin from random coil to  $\beta$ -sheet conformation (Freddi et al., 1999; Um et al., 2001; Ha et al., 2003), which increases the crystallinity and diminishes the water solubility of the treated samples. Solvent exposition is known also to induce silk fibroin gelation (De Moraes et al., 2015). Gels are stabilized by the formation of 240 thermodynamically stable  $\beta$ -sheets, which serve as physical cross-links to stabilize gels and are essentially irreversible under physiological conditions, unless degraded due to enzymatic or oxidative processes. Conversely, in this work we demonstrated that a reversible silk fibroin sol-gel transition can be induced by applying a mechanical stress (i.e. agitation) on a hydro-alcoholic dispersion of silk fibroin probably because of the presence of glycerin.

245 This particular composition appears useful to design in situ film forming formulations intended to be applied on the skin. As a matter of fact, such a type of dosage forms is usually based on a combination of volatile solvents that allow the fast formation of the film onto the skin. Moving from organic solvents to water, the drying time would become slower and consequently the residence time of the wet formulation could become critical. The use of thixotropic gels can overcome these potential issues since the

250 formulations can be easily applied onto the skin using a roller or a spray and the fast recover of their consistence after application reduces the risk of lack of uniformity of the film during drying.

In conclusion, hydro-alcoholic silk fibroin gels plasticized with glycerin could be advantageously used to prepare in situ film forming dosage forms intended for a cutaneous administration.

## References

- Cilurzo, F., Alberti, E., Minghetti, P., Gennari, C.G.M., Casiraghi, A., Montanari, L., 2010. Effect of drug chirality on the skin permeability of ibuprofen. *Int. J. Pharm.* 386 (1-2), 71-76.
- Cilurzo, F., Casiraghi, A., Selmin, F., Minghetti, P., 2015. Supersaturation as a tool for skin penetration enhancement. *Curr. Pharm. Design.* 21 (20), 2733-2744.
- Cilurzo, F., Selmin, F., Gennari, C.G.M., Montanari, L., Minghetti, P., 2014. Application of methyl methacrylate copolymers to the development of transdermal or loco-regional drug delivery systems. *Exp. Op. Drug Del.*, 11(7), 1033-45.
- Dai, L., Li, J., Yamada, E., 2002. Effect of glycerin on structure transition of PVA/SF blends. *J. Appl. Polym. Sci.* 86, 2342-2347.
- De Moraes, M.A., Mahl, C.R.A., Silva, M.F., Beppu, M.M., 2015. Formation of silk fibroin hydrogel and evaluation of its drug release profile. *J. Appl. Polym.Sci.*, 132 (15), DOI: 10.1002/APP.41802.
- EMA/CHMP/QWP/608924/2014. Guideline on quality of transdermal patches, 2014.
- Franzè, S., Gennari, C.G., Minghetti, P., Cilurzo, F., 2015. Influence of chemical and structural features of low molecular weight heparins (LMWHs) on skin penetration. *Int. J. Pharm.* 481 (1-2), 79-83.
- Freddi, G., Pesina, G., Tsukada, M., 1999. Swelling and dissolution of silk fibroin (*Bombyx mori*) in N-methyl morpholine N-oxide. *Int. J. Biol. Macromol.* 24, 251-263.
- Gennari, C.G.M., Franzé, S., Pellegrino, S., Corsini, E., Vistoli, G., Montanari, L., Minghetti, P., Cilurzo, F., 2016. Skin penetrating peptide as a tool to enhance the permeation of heparin through human epidermis. *Biomacromol.* 17(1), 46-55.
- Ha, S.W., Park, Y.H., Hudson, S.M., 2003. Dissolution of *Bombyx mori* silk fibroin in the calcium nitrate tetrahydrate–methanol system and aspects of wet spinning of fibroin solution. *Biomacromol.* 4, 488–496.
- Hofmann, S., Wong Po Foo, C.T., Rossetti, F., Textor, M., Vunjak-Novakovic, G., Kaplan, D.L., Merkle, H.P., Meinel, L., 2006. Silk fibroin as an organic polymer for controlled drug delivery. *J. Control. Rel.* 111, 219–227.
- Jin, H. J., Park, J., Karageorgiou, V., Kim, U.J., Valluzzi, R., Cebe, P., Kaplan, D. L., 2005. Water-insoluble silk films with reduced  $\beta$ -sheet content. *Adv. Funct. Mater.* 15, 1241-1247.

Kawahara, Y., Furukawa, K., Yamamoto, T., 2006. Self-Expansion Behavior of Silk Fibroin Film. *Macromol. Mater. Eng.*, 291, 458-462.

Kim, J.I. and Choi, H.K., 2002. Effect of additives on the crystallization and the permeation of ketoprofen from adhesive matrix. *Int. J. Pharm.* 236, 81--85.

Kim, U.J., Park, J., Li, C., Jin, H.J., Valluzzi, R., Kaplan, D.L., 2004. Structure and properties of silk hydrogels. *Biomacromol.* 5, 786–92.

Lu, S., Wang, X., Lu, Q., Zhang, X., Kluge, J. A., Uppal, N., Omenetto, F., Kaplan, D. L., 2010. Insoluble and flexible silk films containing glycerol. *Biomacromol.* 11, 143-150.

Matsumoto, A., Chen, J., Collette, A.L., Kim, U.J., Altman, G.H., Cebe, P., 2006. Mechanisms of silk fibroin sol–gel transitions. *J Phys Chem B* 110, 21630–21638.

Minghetti, P., Cilurzo, F., Pagani, S., Casiraghi, A., Assandri, R., Montanari, L., 2007. Formulation study of oxybutynin patches. *Pharm. Dev. Technol.* 12 (3), 239-246.

**Nazarov, R., Jin, H.J., Kaplan, D.L., 2004. Porous 3-D Scaffolds from Regenerated Silk Fibroin, *Biomacromol.* 5 (3), 718–726.**

OECD Guideline for the testing of chemicals – Skin Absorption: in vitro methods. 428. Adopted 13 april 2004

Pritchard E.M., Valentin T., Panilaitis B., Omenetto F., Kaplan D.L. 2013. Antibiotic- releasing silk biomaterials for infection prevention and treatment, *Adv. Funct. Mater.* 23, 854–861.

Selmin, F., Gennari, C.G.M., Minghetti, P., Marotta, L.A., Viviani, B., Vagdama, P., Montanari, L., Cilurzo, F., 2014. Enhanced hydration stability of *Bombix mori* silk fibroin/PEG 600 composite scaffolds for tissue engineering. *Polym. Advan. Technol.* 25 (5), 532-538.

Um, I.C., Kweon, J.Y., Park, Y.H., Hudson, S., 2001. Structural characteristics and properties of the regenerated silk fibroin prepared from formic acid. *Int. J. Biol. Macromol.* 29, 91–97.

van de Sandt, J.J.M., van Burgsteden, J.A., Cage, S., Carmichael, P.L., Dick, I., Kenyon, S., Korinth, G., Larese, F., Limasset, J.C., Maas, W.J.M., Montomoli, L., Nielsen, J.B., Payan, J.-P., Robinson, E., Sartorelli, P., Schaller, K.H., Wilkinson, S.C., Williams, F.M., 2004. In vitro predictions of skin absorption of caffeine, testosterone, and benzoic acid: a multi-centre comparison study. *Regul. Toxicol. Pharmacol.* 39(3), 271–281.

**Vepari, C. and Kaplan, D.L., 2007. Silk as a biomaterial. Prog. Polym. Sci. 32, 991–1007.**

Wang, H., Zhang, Y., Shao, H., Hu X., 2005. A study on the flow stability of regenerated silk fibroin aqueous solution. *Int. J. Biol. Macromol.* 36, 66–70.

Wang, X., Zhang, X., Castellot, J., Herman, I., Iafrati, M., Kaplan, D., 2008. Controlled release from multilayer silk biomaterial coatings to modulate vascular cell responses. *Biomater.* 29, 894– 903.

## Figure captions

**Figure 1:** Stress-strain graph for textural profile of formulation G7.

**Figures 2:** Main textural parameters: a) cohesiveness (AUC+), b) hardness ( $\sigma_{\max}$ ) and c) adhesiveness ( $\sigma_{\min}$ ) of gels as a function of silk fibroin and ethanol concentrations. The axes have been arranged to best show the effects on textural parameters.

**Figures 3:** Main textural parameters: a) cohesiveness (AUC+), b) hardness ( $\sigma_{\max}$ ) and c) adhesiveness ( $\sigma_{\min}$ ) of gels as a function of silk fibroin and glycerin concentrations. The axes have been arranged to best show the effects on textural parameters.

**Figure 4:** Rheological curves of formulation G4 showing the thixotropic behavior of the sample. Black curve was obtained starting the analysis at low shear rates; dotted curve was obtained immediately after on the same sample passing from high to low shear rates.

**Figure 5:** Caffeine permeation from silk fibroin films and reference solution (1% w/w caffeine) through human epidermis.

**Table 1** – Silk fibroin gel composition and their main technological properties: effect of silk fibroin and ethanol concentrations.

Form code	Silk fibroin (% w/v)	Silk fibroin solution/ EtOH ratio	Gly (% w/w)	Spreadability	$\sigma_{\max}$ (kPa)	AUC+ (mJ)	$\sigma_{\min}$ (kPa)	$t_{ev}$ (min)
A1	0.6	30/70	--	B	$0.474 \pm 0.041$	$0.045 \pm 0.007$	$0.165 \pm 0.015$	$7 \pm 3$
A2	1.0	50/50	--	B	$1.565 \pm 0.457$	$0.128 \pm 0.027$	$0.465 \pm 0.045$	$23 \pm 2$
A3	1.4	70/30	--	B	$0.447 \pm 0.088$	$0.024 \pm 0.008$	$0.178 \pm 0.027$	$21 \pm 2$
A4	0.9	30/70	--	B	$0.887 \pm 0.215$	$0.080 \pm 0.007$	$0.311 \pm 0.013$	$8 \pm 3$
A5	1.5	50/50	--	C	$2.081 \pm 0.255$	$0.210 \pm 0.016$	$0.697 \pm 0.066$	$36 \pm 6$
A6	2.1	70/30	--	C	$1.556 \pm 0.511$	$0.166 \pm 0.049$	$0.487 \pm 0.097$	$37 \pm 9$
A7	1.2	30/70	--	C	$1.242 \pm 0.319$	$0.134 \pm 0.032$	$0.515 \pm 0.064$	$35 \pm 3$
A8	2.0	50/50	--	C	$3.329 \pm 1.109$	$0.356 \pm 0.073$	$0.939 \pm 0.237$	$55 \pm 3$
A9	2.8	70/30	--	C	$4.102 \pm 0.211$	$0.525 \pm 0.039$	$1.288 \pm 0.215$	$39 \pm 11$



**Table 2** – Equations obtained by multiple regression to evaluate the effect of the two formulative variables, namely sf and ethanol (EtOH) concentrations on hardness ( $\sigma_{max}$ ), cohesiveness ( $AUC+$ ) and adhesiveness ( $\sigma_{min}$ ) of silk fibroin gels.

Equation	R <sup>2</sup>	F Value	Prob>F
$\sigma_{min} = -1.061 \pm 0.424 + 0.674 \pm 0.128 SF + 0.012 \pm 0.005 EtOH$	0.85	16.631	0.003
$AUC+ = -0.513 \pm 0.175 + 0.296 \pm 0.053 SF + 0.005 \pm 0.002 EtOH$	0.86	19.230	0.002
$\sigma_{max} = -3.432 \pm 1.612 + 2.211 \pm 0.488 SF + 0.03716 \pm 0.01947 EtOH$	0.81	12.846	0.006

**Table 3** – Silk fibroin gel composition and their main technological properties: effect of the plasticizer, namely glycerin. All formulations were prepared with the largest amount of ethanol.

Form code	Silk fibroin (% w/v)	Gly (% w/w)	Silk fibroin/ Gly ratio	Spreadability		$\sigma_{\max}$ (kPa)	AUC+ (mJ)	$\sigma_{\min}$ (kPa)	(n)
				Before agitation	After agitation				
G1	0.6	2.5	0.24	B	A	0.453 ± 0.037	0.042 ± 0.007	0.150 ± 0.011	1
G2	0.6	5	0.12	B	C*	1.000 ± 0.076	0.064 ± 0.006	0.124 ± 0.034	1
G3	0.6	7.5	0.08	B	C*	0.949 ± 0.165	0.067 ± 0.001	0.157 ± 0.039	1
G4	0.9	2.5	0.36	B	A	2.219 ± 0.834	0.131 ± 0.015	0.217 ± 0.056	1
G5	0.9	5	0.18	B	A	2.610 ± 0.152	0.148 ± 0.010	0.299 ± 0.038	1
G6	0.8	7.5	0.11	B	C*	2.126 ± 0.267	0.143 ± 0.004	0.249 ± 0.000	1
G7	1.2	2.5	0.48	C	-	2.493 ± 0.100	0.181 ± 0.008	0.609 ± 0.006	1
G8	1.1	5	0.22	B	A	2.894 ± 0.400	0.219 ± 0.005	0.267 ± 0.058	1
G9	1.1	7.5	0.15	B	A	3.707 ± 0.149	0.216 ± 0.001	0.270 ± 0.045	2

\* The score was considered C due to shrinkage of the formulation after spreading onto the release liner.

**Table 4** – Skin permeation parameter of caffeine released from in situ film formed films, pre-formed film and reference solution (mean±standard deviation, n=3).

<b>Formulation</b>	<b>J<sub>max</sub> (<math>\mu\text{g}/\text{cm}^2/\text{h}</math>)</b>	<b>Lag Time (h)</b>
<b>G1</b>	1.36 ± 0.34	2.9 ± 0.8
<b>G4</b>	1.41 ± 0.36	3.4 ± 0.7
<b>G5</b>	1.74 ± 0.33	1.3 ± 0.8
<b>G5 pre-formed film</b>	1.62 ± 0.30	2.3 ± 0.3
<b>hydro-alcoholic solution</b>	0.84 ± 0.06	5.4 ± 0.1

Figure 1: Stress-strain graph for textural profile of formulatio

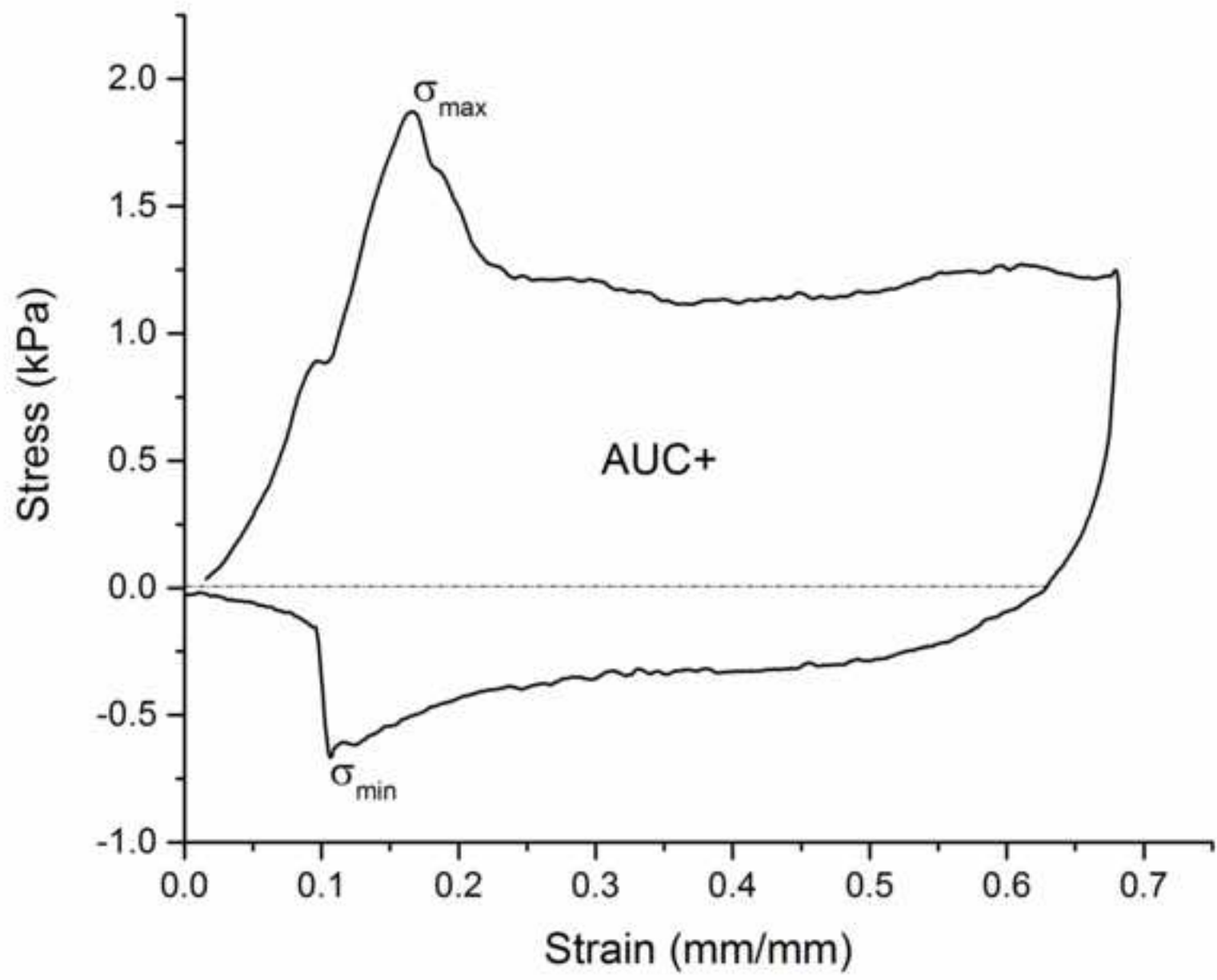


Figure 2a

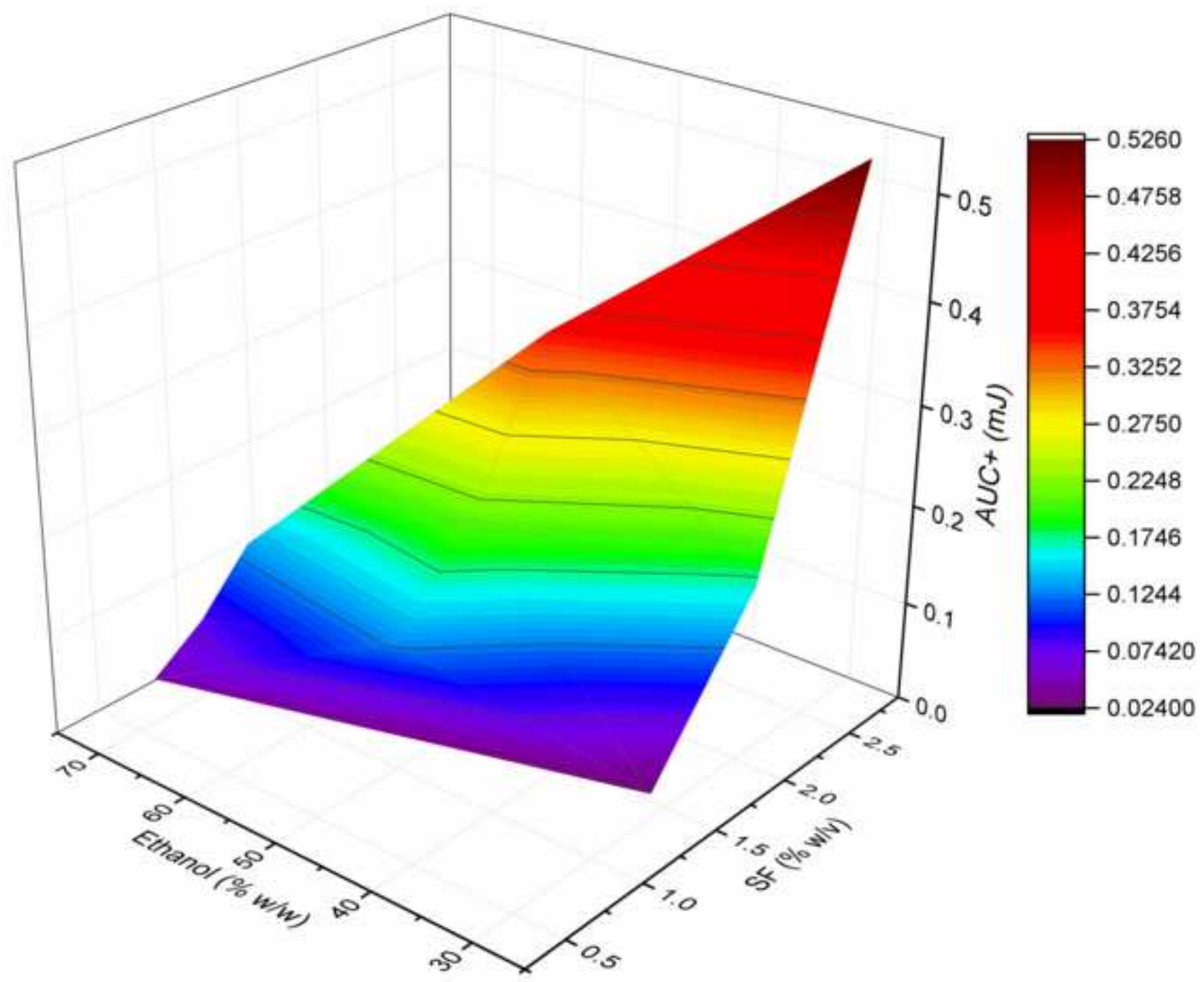


Figure 2b

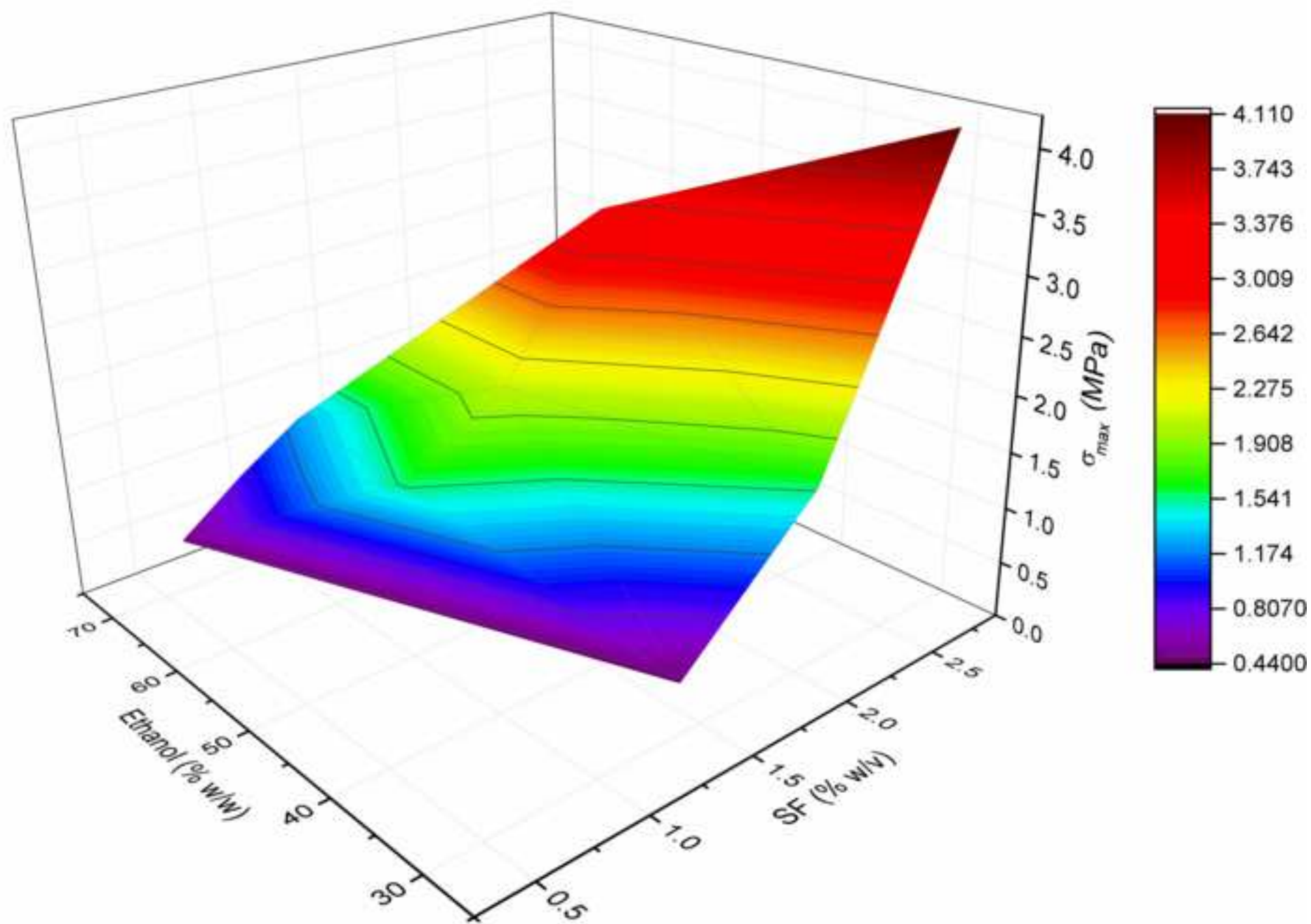


Figure 2c

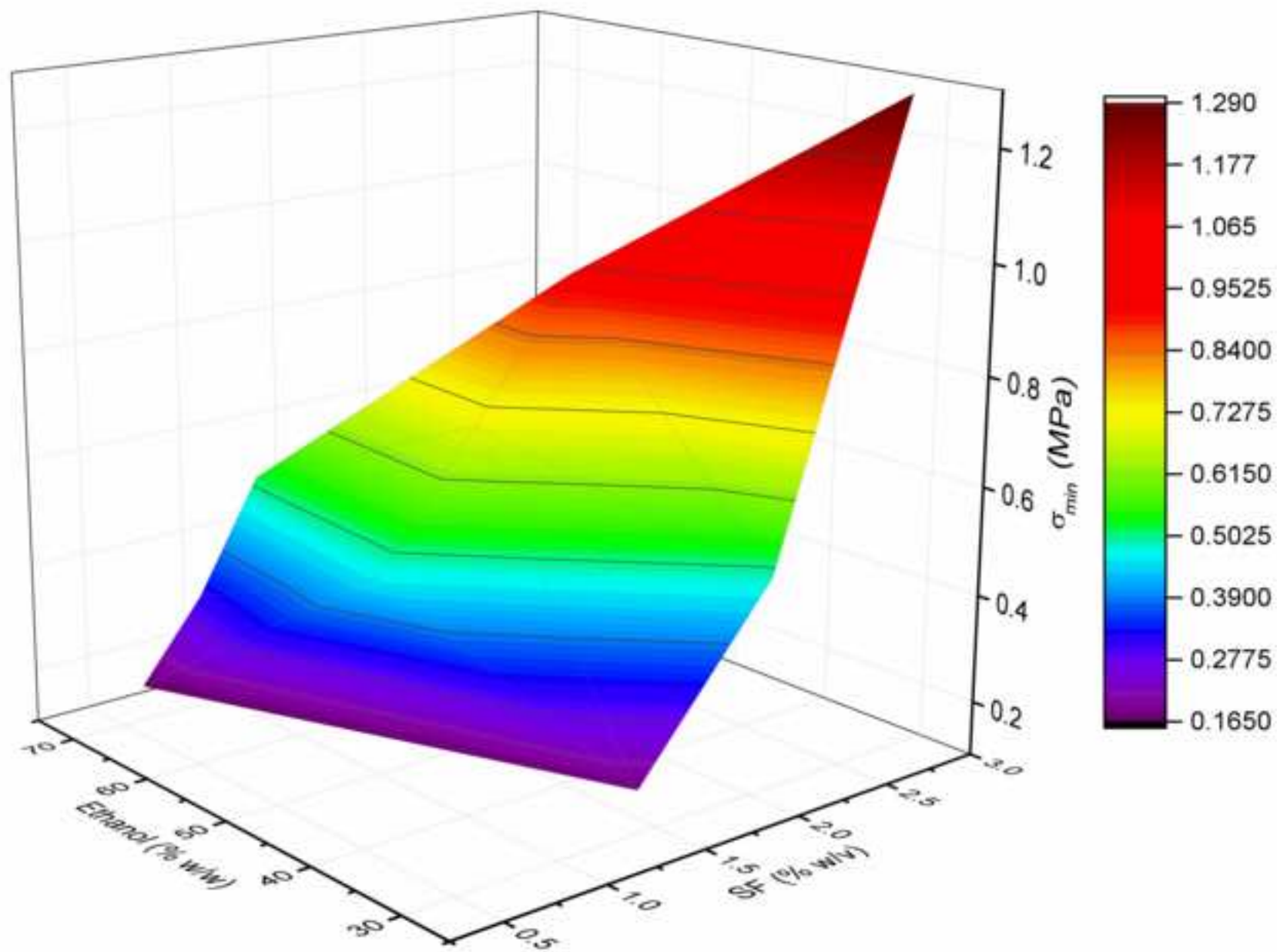


Figure 3a

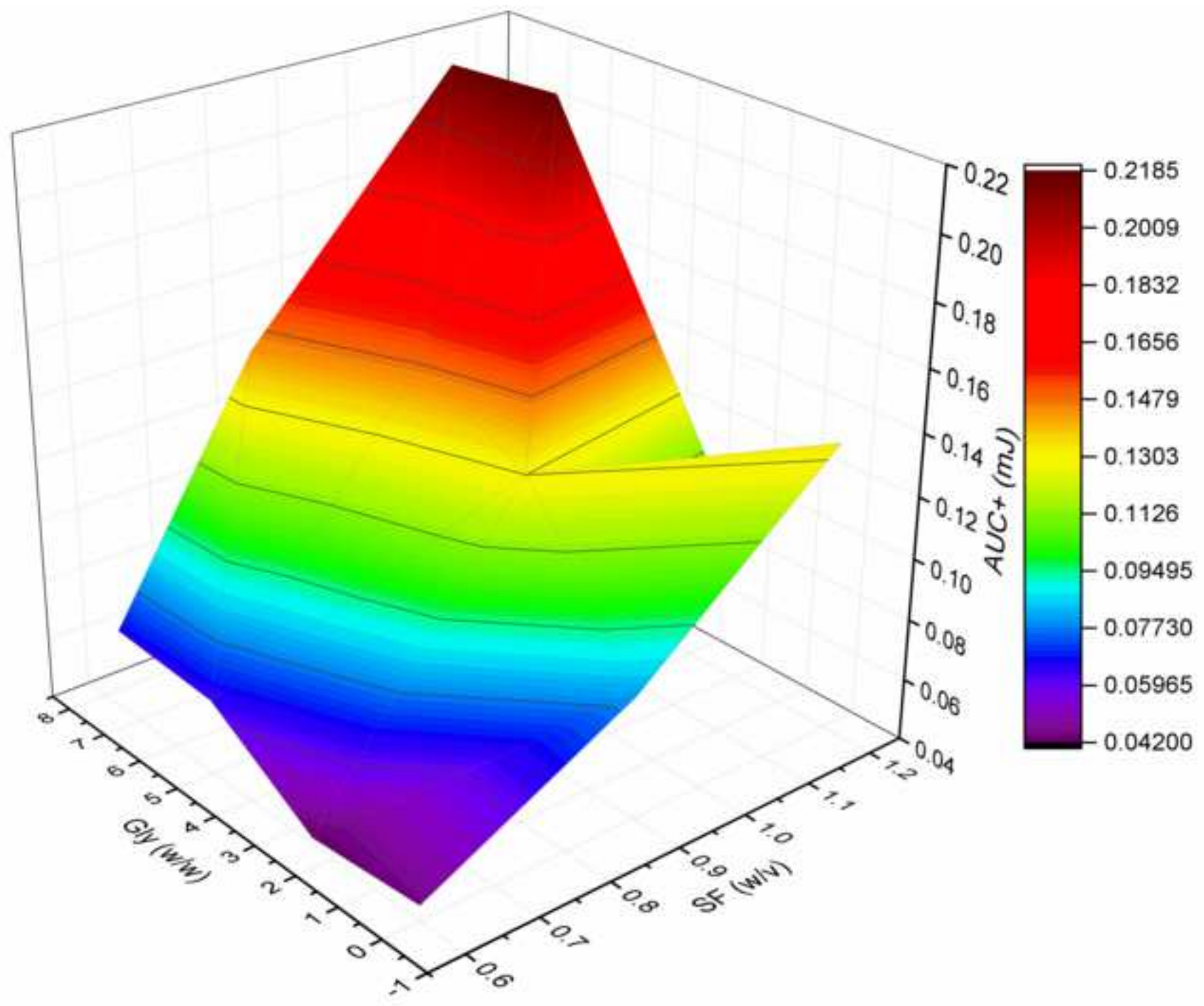




Figure 3b

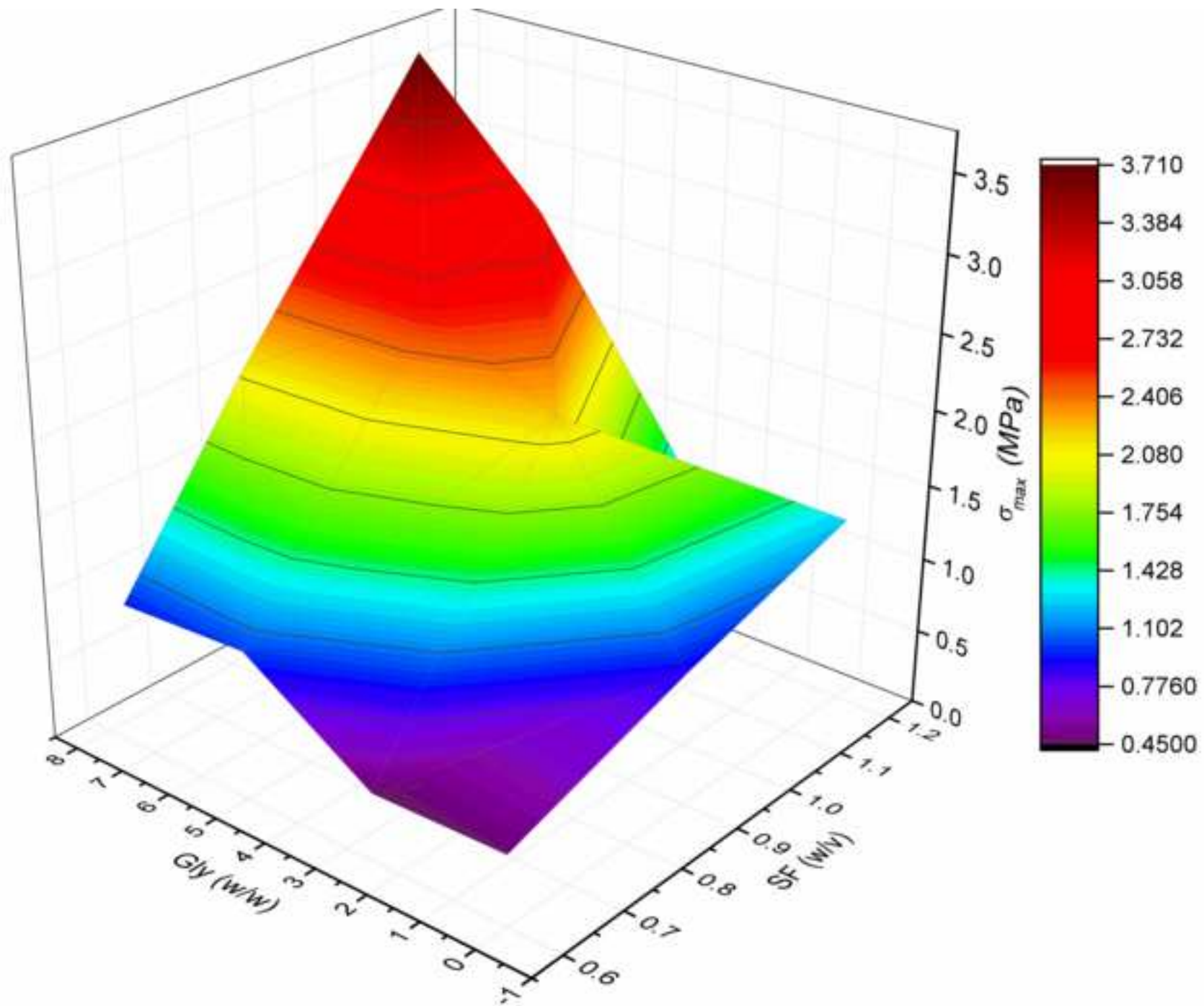


Figure 3c

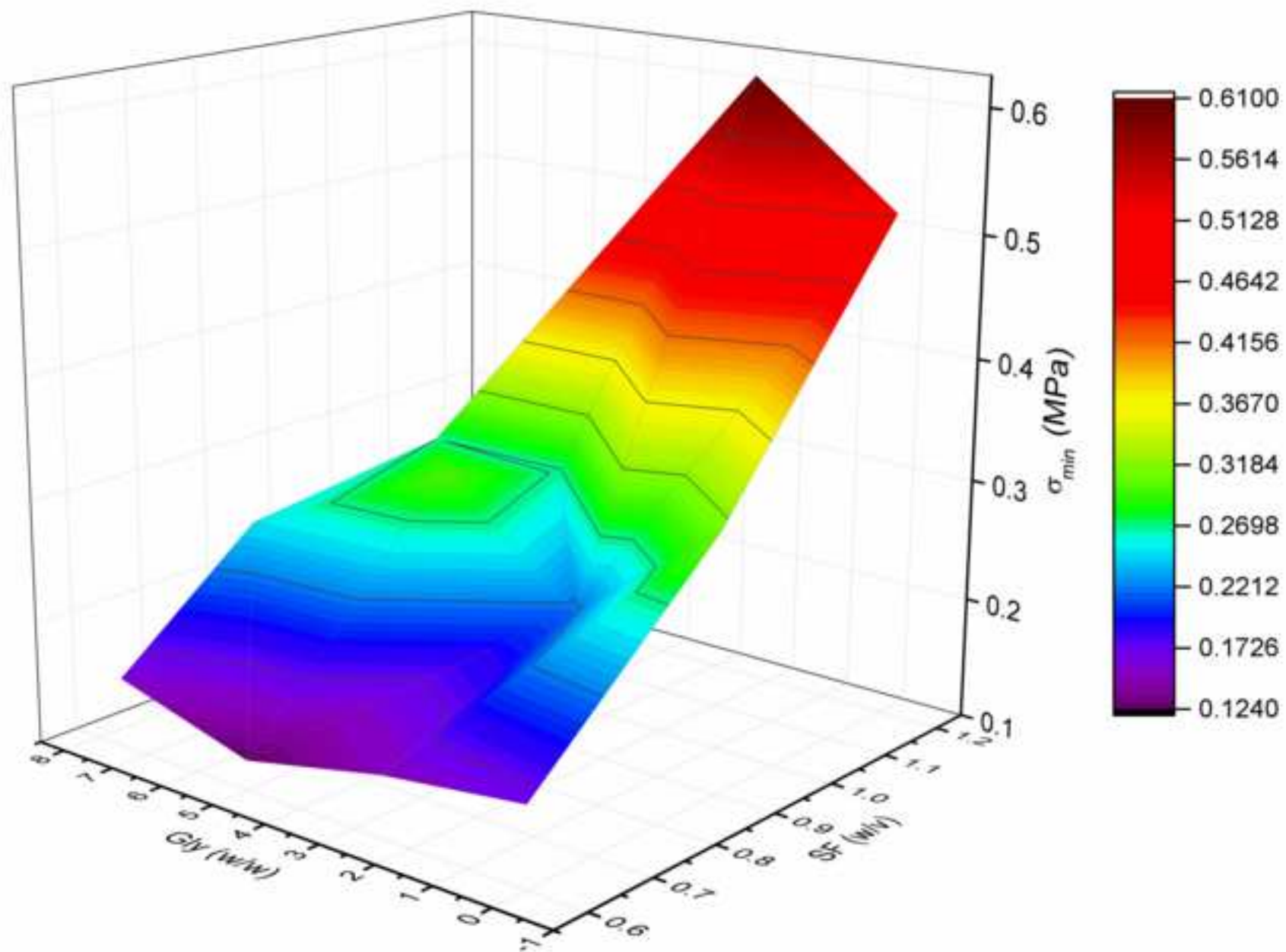


Figure 4

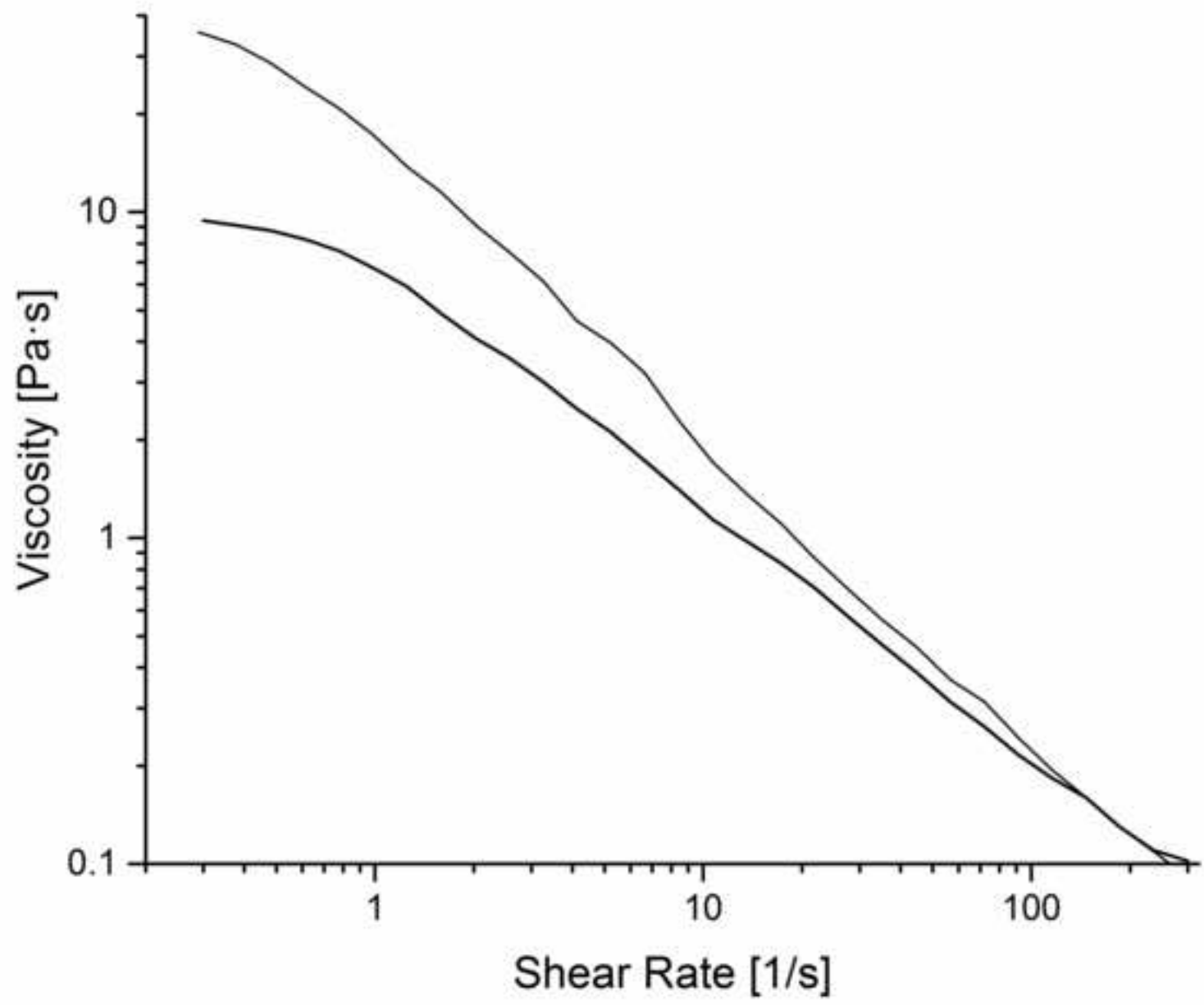


Figure 5

